

Influence of electrolyte additives on the performance of the positive plates of lead batteries

A. Aleksandrova*, M. Matrakova, P. Nikolov

Institute of Electrochemistry and Energy Systems "Acad. Evgeni Budevski", Bulgarian Academy of Sciences, Acad. Georgi Bonchev Str., 1113 Sofia, Bulgaria

Received: November 17, 2021; Revised: February 28, 2022

In this work, different concentrations of sodium dodecyl sulfate (SDS) or cetyltrimethylammonium bromide (CTAB) were used as electrolyte additives in flooded laboratory test lead acid cells with 2 positive and 3 negative plates to evaluate the influence of the selected additives on the cycling performance of the positive plates at 17.5% DoD (depth-of-discharge) employing PSoC (partial state-of-charge) cycling protocol for automotive applications. On the basis of the obtained results the optimal concentrations of the tested surfactants SDS or CTAB in the electrolyte were established as follows: 600 ppm SDS and 100 ppm CTAB. These concentrations of the additives under test exert strong influence on the size of the individual PbO_2 particles, the volume of pores and the pore surface area. The experimental results demonstrate that the selected organic substances are promising for use as electrolyte additives for lead batteries that operate under partial-state-of-charge conditions.

Keywords: lead acid battery, positive electrode, positive active mass, surfactant, PSoC cycling, electrolyte additive

INTRODUCTION

New applications such as micro-hybrid cars, remote telecommunications and energy storage for renewables are placing strong demands upon lead acid batteries for improved charge-acceptance and extended service life under partial state-of-charge (PSoC) conditions. The main processes that lead to decline of the capacity and the cycle endurance of lead acid batteries are irreversible formation of PbSO_4 in the negative active mass (NAM), corrosion of positive electrode grids, positive active mass (PAM) degradation, loss of adherence to the grid and shedding, hydrogen and oxygen evolution reactions, etc. [1]. In the past decade the problems of NAM performance under PSoC cycling conditions were largely overcome by addition of carbon materials in the negative electrodes. Hence, the positive electrodes could become the limiting factor for further improvement of the cycling endurance of lead batteries. PAM has a complex structural organization – the very fine individual PbO_2 particles are interconnected into agglomerates which in turn are organized in aggregates. These structural elements form the pore system of PAM – comprising reaction and transport pores. The individual PbO_2 particles themselves have a complex structure consisting of gel and crystalline zones ensuring proton and electron conductivity, respectively. The equilibrium between the gel and crystalline zones is one of the key factors determining the discharge performance of PAM. In addition, the PbO_2 phase in PAM is present in two

polymorphic forms, alpha- and beta- PbO_2 , which in turn have different crystal morphology and electrochemical behavior [2]. One successful approach employed in lead battery science and technology to improve the capacity and cycle life or suppress the gas evolution reactions is the application of a variety of organic or inorganic substances as additives to the sulfuric acid electrolyte [3–16].

Surfactants are substances that modify the morphology and surface of crystals and can suppress gas evolution, and are widely used in different types of batteries. The influence of surfactants in an electrolyte on the structure and performance of PbO_2 electrodes for wastewater treatment has been extensively investigated in the literature [17–21]. Xiaoliang *et al.* studied the impact of sodium dodecyl sulfate (SDS) on the electro-catalytic performance and the stability of PbO_2 electrode and reported its beneficial effect [20]. Xiaoyue and co-workers used cetyltrimethylammonium bromide (CTAB) or lauryl benzene sulfonic acid sodium into the electrodeposition solution to prevent the aggregation of CNT and assist the doping of CNT into the PbO_2 film [22]. Ghavami *et al.* investigated the effect of surfactants on the sulfation of lead acid cell negative electrodes in high-rate-partial-state-of-charge (HRPSoC) duty and reported that SDS improved the cycle life and fine PbSO_4 crystals were formed, while CTAB surfactant exerted the opposite effect on the crystal morphology of the negative active mass [23]. Nikolov *et al.* [24]

* To whom all correspondence should be sent:
E-mail: albena.aleksandrova@iees.bas.bg

discussed the structural changes in the positive active mass during PSoC operation and the influence of electrolyte additives on the cycling endurance of lead batteries in automotive applications.

In our previous work [25, 26] we presented the obtained results about the effect of SDS or CTAB on the electrochemical behavior of lead acid battery alloys.

The focus of the present study is to evaluate the structural changes of the positive active mass during partial state-of-charge operation of lead batteries for automotive applications and to explore the effect of SDS or CTAB as additives to the sulfuric acid electrolyte solution aimed to improve the cycling performance of PAM.

EXPERIMENTAL

Materials

In this work, two types of surfactants, anionic sodium dodecyl sulphate (SDS) and cationic cetyltrimethylammonium bromide (CTAB), were used as electrolyte additives in lead test cells. Sulfuric acid (95-98%), SDS (> 98.5%) and CTAB (> 99%) were supplied by Sigma-Aldrich. Three concentrations of the additives in $1.28 \text{ cm}^3 \cdot \text{g}^{-1}$ H_2SO_4 aqueous solution were tested, as follows: 240 ppm, 600 ppm and 1200 ppm of SDS; and 100 ppm, 240 ppm and 500 ppm of CTAB, respectively.

Electrodes manufacture and test cell design

Positive and negative paste batches were produced using ball mill type leady oxide. The negative paste composition was as follows: 0.5 wt.% carbon material (PBX51, Cabot Corp. (USA)), 0.2 wt.% lignosulfonate additive (Vanisperse-A, Borregaard LignoTech (USA)) and 0.8 wt.% BaSO_4 (Blank Fixe N, Solvay, (Belgium)) The positive paste contained no additives. The thus produced positive and negative pastes were used for pasting small Pb-0.06Ca-1.25Sn alloy grids marked as PbCa grids. The positive plates were wrapped in polyethylene separator (Daramic (USA)) with ribs facing the negative plates. Flooded laboratory test cells with 2 positive and 3 negative plates per cell were used to evaluate the influence of the selected electrolyte additives on the electrochemical performance of the positive plates. The obtained plates were subjected to standard and widely accepted by the industry curing, drying and formation processes suitable for 3BS paste technology.

Performance tests and characterization

Testing was conducted using 2V flooded test cells with 2 positive and 3 negative plates per cell and rated (nominal) capacity of 4.0 Ah at 20 h rate of discharge and 50% utilization of the positive active mass (PAM). Thus, the performance parameters of the cells were limited by the positive plates. Each investigated surfactant was dissolved in $1.28 \text{ cm}^3 \cdot \text{g}^{-1}$ H_2SO_4 solution and after complete formation of both the positive and negative electrodes, the cells were refilled with doped solutions. Control cells (blank) with no additives to the electrolyte were also assembled. Initial capacity tests comprising three consecutive C_{20} (the energy a battery can deliver continuously for 20 hours) discharge-charge cycles were performed and after that the test cells were subjected to cycling endurance test at 17.5% DoD (depth-of-discharge) according to the EN 50324-6 protocol, but without capacity checks after every 85 cycles. All above mentioned tests were performed at a temperature of 25°C . At the end-of-life of each of test cells, the cell was disassembled and the positive and negative plates were washed under running water. The positive plates were dried in a thermo-chamber, while the negative plates were immediately put in and dried in thermo-chamber under nitrogen atmosphere in order to avoid oxidation of the negative active mass (NAM).

The powder X-ray diffraction patterns of the tested active masses were recorded on an X-ray diffractometer APD 15 Philips 2134 (Cu $K\alpha$ radiation). The structure and crystal morphology of the active masses was observed on a JEOL 200 CX scanning electron microscope. The samples taken from the cells under test were set also to Hg porosimetry (MICROMERITICS AutoPore 9200) to estimate the pore volume distribution by pore radius of the positive active masses.

RESULTS AND DISCUSSION

Figure 1 presents the results of the initial C_{20} capacity tests of lead cells with different concentrations of the tested surfactants in the electrolyte. The obtained results indicate that, in the case of cells with SDS doped electrolyte, increase of SDS concentration results in reduction of C_{20} discharge capacity by about 15%. Addition of CTAB to the electrolyte has a negligible effect on C_{20} discharge capacity. All tested cells exhibit a progressive decline in C_{20} discharge capacity from cycle to cycle, except the blank cell. Yet, all tested cells have higher initial capacities than the rated values and exhibit C_{20} capacity performance better than 120% of the nominal capacity value.

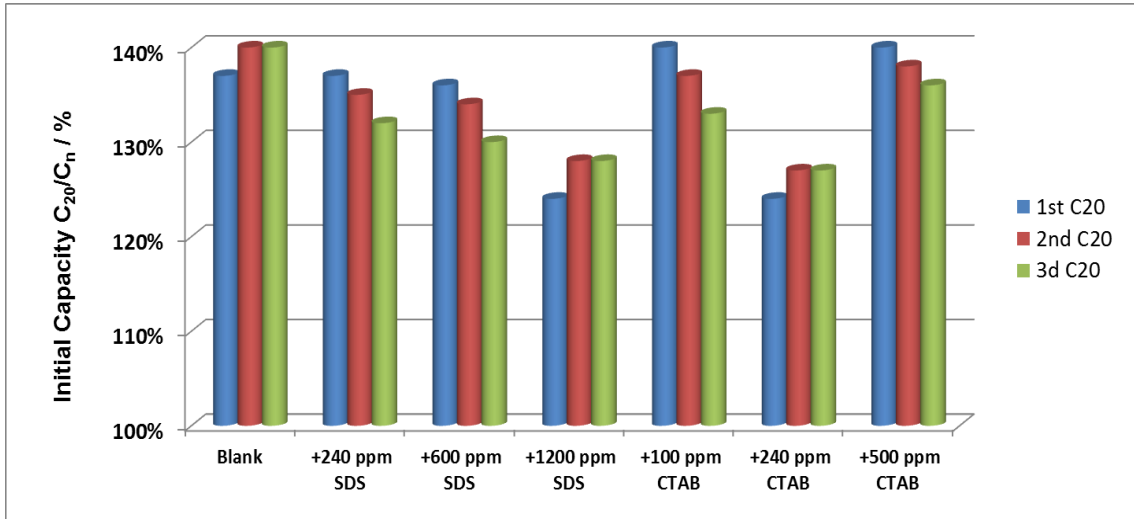


Figure 1. Initial C₂₀ capacities of test cells with blank or surfactant-doped solutions. Values are reported as percent of actual versus rated discharge capacity.

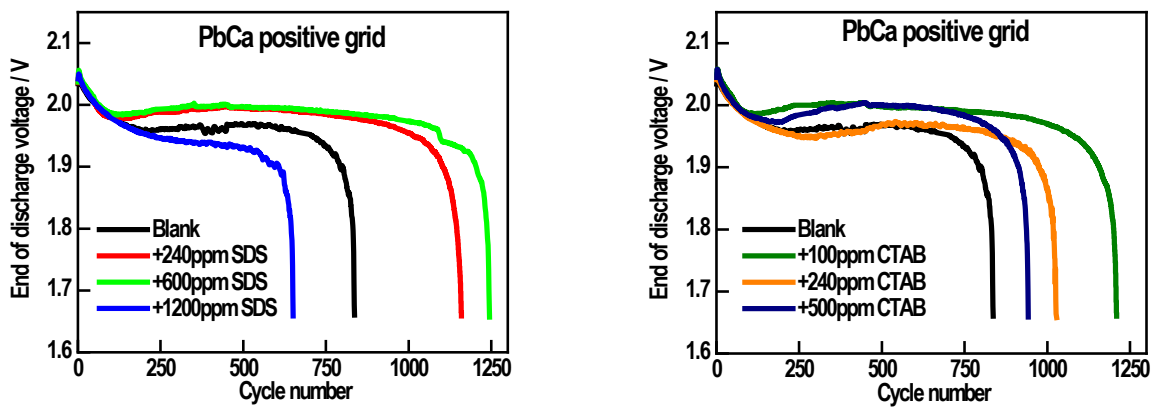


Figure 2. Changes in end-of-discharge voltage of test cells with different electrolyte additives cycled continuously with 17.5% DoD.

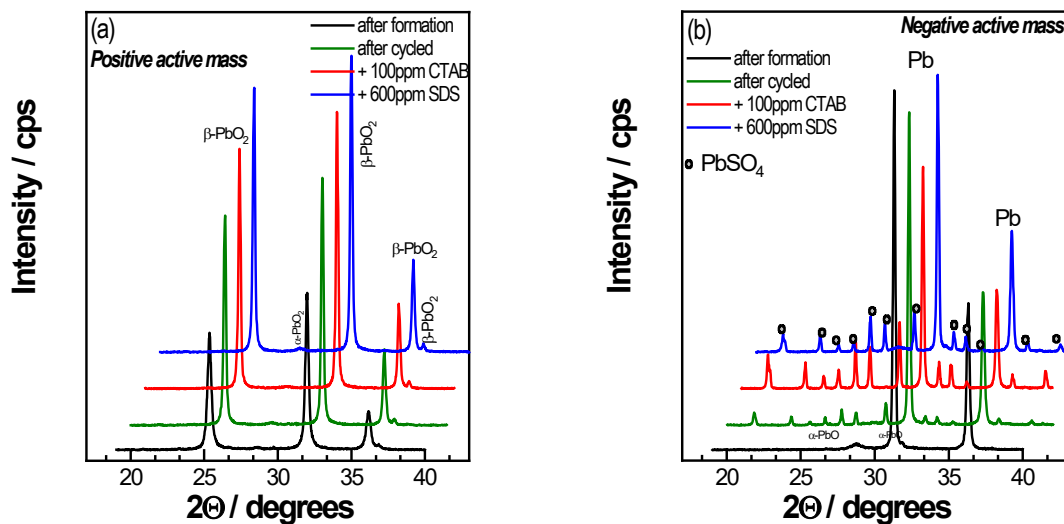


Figure 3. XRD patterns of different active mass samples after the cycling test: (a) PAM and (b) NAM.

Figure 2 illustrates the end-of-discharge voltage course during the cycling test of the cells containing the studied additives in the electrolyte. The cut-off voltage limit of the test was 1.65V.

The experimental results evidence that the cell with blank electrolyte endures 800 cycles. The differences in end-of-discharge voltage course during PSoC cycling suggest that SDS and CTAB

and their loading concentrations have their own specific effect on the processes in PAM. The left-hand figure shows that the dependence of the number of completed PSoC cycles as a function of dosage levels of SDS in the electrolyte passes through a maximum at 600 ppm additive load. Increase of CTAB concentration in the cell electrolyte above 100 ppm has negative impact on PSoC cycling endurance.

The phase composition of freshly formed and cycled PAM and NAM samples was determined by X-ray diffraction analysis. Figure 3 summarizes the XRD patterns recorded for NAM and PAM samples taken from the blank and the best performed doped test cells.

The intensity of the beta-PbO₂ [1 1 0] and [0 1 1] peaks is affected by both, the number of completed cycles and the type of studied electrolyte additives. The obtained XRD patterns of the cycled PAM samples taken from different test cells evidence that these peaks have twice higher

intensity than that of the freshly formed PAM sample.

As can be seen from the data in Fig.3b, the NAM sample taken from the cycled blank cell contains the lowest amount of PbSO₄. This finding is related to the smallest number of completed cycles during the PSoC cycling test. The XRD peaks of lead sulfate phase for NAM samples cycled in the presence of 100 ppm CTAB or 600 ppm SDS have more than twice higher intensity. Yet, these are the cells that endure the highest number of PSoC cycles. As is well known, in battery applications under PSoC conditions, insoluble PbSO₄ crystals accumulate on the surface of the negative electrodes.

The effect of number of completed PSoC cycles and studied electrolyte additives on PAM and NAM morphology was observed by scanning electron microscopy. Figure 4 compares the microstructure of the positive plate interior of freshly formed and cycled PAM samples at two different magnifications.

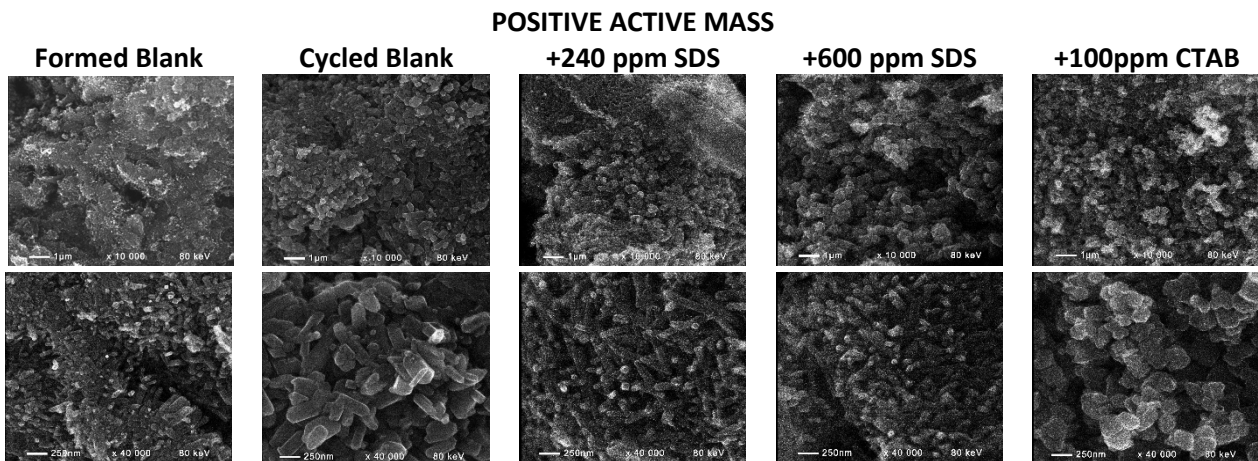


Figure 4. Scanning electron microscopy images of freshly formed and cycled PAM samples taken from different test cells.

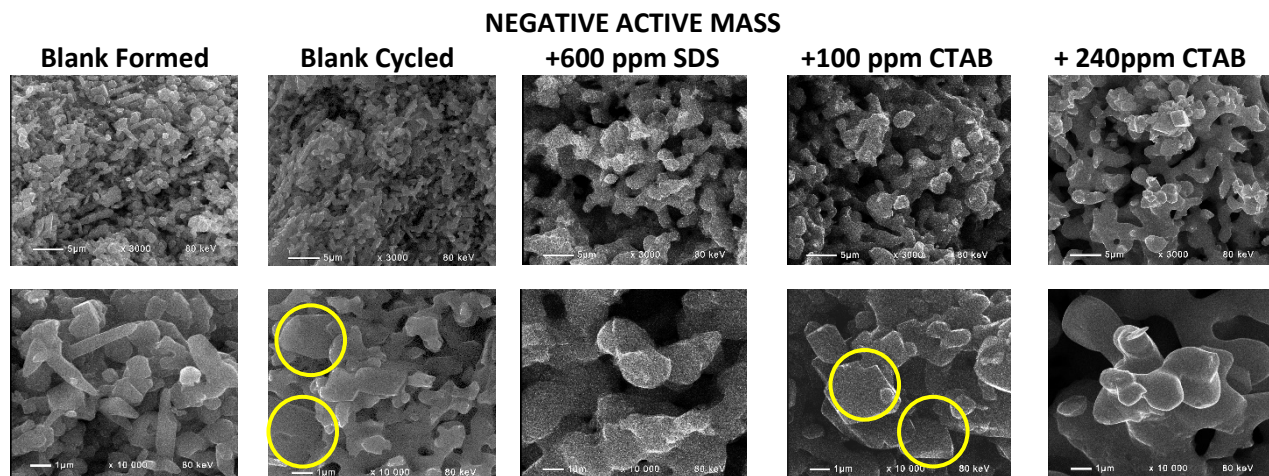


Figure 5. Scanning electron microscopy images of freshly formed and cycled NAM samples taken from different test cells. The yellow circles on the images mark PbSO₄ crystals in the NAM interior.

The SEM images of the freshly formed PAM sample feature very fine individual needle-like PbO_2 particles (about few nm in size), tightly interconnected in agglomerates (1-2 μm in size), which in turn are grouped together into aggregates (10-20 μm in size). The morphology of the cycled blank PAM samples differs completely. The individual PbO_2 particles are rounded in shape and much bigger in size (100-500 nm) and the connection between the particles is loose. The crystal morphology of PAM samples cycled in the presence of 240 ppm CTAB or 600 ppm of SDS features fine individual stick-like PbO_2 particles (200-250 nm in length). Analogous effect of SDS on the microstructure of PbO_2 crystals was mentioned by Xiaoliang *et al.* and Amadelli *et al.* when modified PbO_2 electrode was synthesized by electro-deposition method. [20, 27]. O. Shmychkova *et al.* and R. Munoz-Espi *et al.* have explained that surfactant additives selectively adsorb on the surface and reduce the growth of crystals and thereby alter their shape and size [28, 29].

The morphology of PbO_2 crystals of the 100 ppm CTAB PAM sample (Fig. 4) is similar to that of the cycled blank sample. The most significant visible difference is the presence of well-formed pores between the aggregates in the interior of the 100 ppm CTAB PAM sample. The sample doped with 240 ppm SDS is characterized by compact structure. The SEM images of PAM samples cycled in the presence of 1200 ppm of SDS or 500 ppm of CTAB feature structures similar to that of the cycled blank sample. Probably, at these higher concentration levels of the additives in H_2SO_4 aqueous solution, the molecules of the tested surfactants self-organize in a supramolecular assembly, as a result of which their influence on the processes of PbO_2 crystallization weakens.

Figure 5 presents scanning electron microphotographs of freshly formed and cycled NAM samples at two different magnifications. The SEM images indicate that, despite the considerable amount of PbSO_4 phase detected in the negative plates by XRD, the NAM interior contains predominantly Pb phase. Hence, it can be assumed that the PbSO_4 crystals are concentrated mainly in regions close to the surface of the negative plate, which is a typical failure mode for lead batteries operated at PSoC conditions. Normally, PbSO_4 crystals are about 5 μm big in size and have well shaped walls, edges, and apexes and sometimes are incorporated in the network structure of Pb. The cycled black NAM sample features very compact structure built of irregularly shaped Pb crystals. The

studied electrolyte additives have similar effect on the morphology of the Pb crystals. Both SDS and CTAB surfactants provoke a change of the typical NAM energetic structure to a more skeleton-like one as observed in the SEM images of the electrolyte doped samples. It is clearly evident that, in the presence of surfactant, the NAM microstructure features significantly higher open porosity as compared to the blank NAM sample.

Hg porosimetry was employed to evaluate the combined effect of the studied additives and the ageing processes due to the employed cycling profile on the characteristics of the PAM pore system. The graphic plots in Figure 6 summarize the cumulative pore volume as a function of the pore radius for PAM samples from the cells with different concentrations of the studied surfactants in the electrolyte.

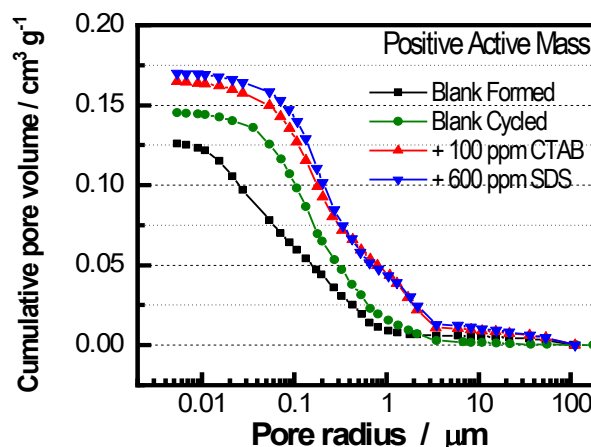


Figure 6. Cumulative pore volume and pore size distribution of different PAM samples obtained by Hg porosimetry.

PSoC cycling with 17.5% DoD has a notable effect on the characteristics of the PAM pore system. The total pore volume of the cycled blank PAM sample increases because of opening of new pores with radii in the range of 0.1 to 1.0 μm as compared to the freshly formed sample. Thus, the ratio of submicron to micron sized pores decreases. This observation is more pronounced for PAM samples cycled in the electrolyte doped with 100 ppm CTAB or 600 ppm SDS.

CONCLUSIONS

On grounds of the obtained results of the present study, it can be concluded that the optimal concentrations of the tested surfactants SDS or CTAB in the electrolyte of lead cells are 600 ppm of SDS and 100 ppm of CTAB. The cells doped with 600 ppm of SDS or 100 ppm of CTAB exhibit an improvement by more than 25% in initial

capacity and cycle life performance vs. the blank electrolyte cell.

Both CTAB and SDS additives exert strong influence on the size of the individual PbO₂ particles. The studied surfactants are promising for use as electrolyte additives for lead batteries that operate under partial-state-of-charge conditions.

REFERENCES

1. P. Ruetschi, *J. Power Sources*, **127**, 33 (2004).
2. D. Pavlov, *Lead-Acid Batteries: Science and Technology*, 2nd edn., Elsevier, 2017.
3. S. Tudor, A. Weisstuch, S. H. Davang, *Electrochem. Technol.*, **5**, 21 (1967).
4. J. Burbank, *J. Electrochem. Soc.*, **111**, 1112 (1964).
5. B. K. Mahato, *J. Electrochem. Soc.*, **126**, 369 (1979).
6. E. Voss, *J. Power Sources*, **24**, 171 (1988).
7. H. A. Laitinen, N. Walkins, *Anal. Chem.*, **47**, 1353 (1975).
8. K. R. Bullock, *J. Electrochem. Soc.*, **126**, 1848 (1979).
9. E. Meissner, *J. Power Sources*, **67**, 135 (1997).
10. K. Saminathan, N. Jayaprakash, B. Rajeswari, T. Vasudevan, *J. Power Sources*, **160**, 1410 (2006).
11. C. Bemelmans, T. O'Keefe, E. Cole, *Bull. Electrochem.*, **12**, 591 (1996).
12. T. C. Wen, M. G. Wei, K. L. Lin, *J. Electrochem. Soc.*, **137**, 2700 (1990).
13. Y. Sato, K. Hishimoto, K. Togashi, H. Yanagawa, K. Kobayakawa, *J. Power Sources*, **39**, 43 (1992).
14. Z. Shi, Y.-H. Zhou, C.-S. Cha, *J. Power Sources*, **70**, 205 (1998).
15. L. Torcheux, C. Rouvet, J. P. Vaurijoux, *J. Power Sources*, **78**, 147 (1999).
16. A. Tizpar, Z. Ghasemi, *Appl. Surface Science*, **252**, 8630 (2006).
17. C. Comninellis, *Electrochim. Acta*, **39**, 1857 (1994).
18. M. Panizza, G. Cerisola, *Chem. Rev.*, **109**, 6541 (2009).
19. J. Niu, Y. Li, E. Shang, Z. Xu, J. Liu, *Chemosphere*, **146**, 526 (2016).
20. L. Xiaoliang, X. Hao, Y. Wei, *J. Alloy. Compd.*, **718**, 386 (2017).
21. N. Boudieb, M. Bounoughaz, A. Bouklachi, *Proc.- Soc. Behav. Sci.*, **195**, 1618 (2015).
22. Xiaoyue D., Fang M., Zhongxin Y., Limin C, Xintong J., *J. Electroanalytical Chemistry*, **677–680**, 90 (2012).
23. R. K. Ghavami, F. Kameli, A. Shirojan, A. Azizi, *J. Energy Storage*, **17**, 170 (2018).
24. P. Nikolov, M. Matrakova, A. Aleksandrova, *Proc. 11th Int. Conference on Lead-Acid Batteries - LABAT'2021(Extended Abstracts)*, 8-11 June, Virtual Conference, 63 (2021).
25. M. Matrakova, A. Aleksandrova, P. Nikolov, O. Saoudi, L. Zerroual, *Bulgarian Chemical Communications*, **52 A**, 74 (2020).
26. O. Saoudi, M. Matrakova, A. Aleksandrova, L. Zerroual, *Arabian Journal of Chemistry*, **13**, 5326 (2020).
27. R. Amadelli, L. Samiolo, A. B. Velichenko, V. A. Knysh, T. V. Luk'yanenko, F. I. Danilov, *Electrochimica Acta*, **54**, 5239 (2009).
28. O. Shmychkova, T. Luk'yanenko, A. Velichenko, *ECS Trans.*, **77**, 1617 (2017).
29. R. Munoz-Espi, Y. Mastai, S. Gross, K. Landfester, *Cryst. Eng. Comm.*, **15**, 2175 (2013).